Phase Behavior of Ionic Microemulsions

H.N.W. Lekkerkerker, W.K. Kegel, and J.Th.G. Overbeek

Van't Hoff Laboratory, Utrecht University, Padualaan 8, 3584 CH Utrecht, The Netherlands

Key Words: Interfaces / Phase Transitions / Microemulsions / Electric Double Layers

Non-polar oils and water can form thermodynamically stable quasi-homogeneous (colloidal) mixtures (called microemulsions) in the presence of relatively large amounts (several %) of ionic surfactants. If the surfactant contains a single hydrocarbon chain (e.g. Sodium Dodecyl Sulphate) the presence of a non-ionic cosurfactant (e.g. hexanol) and electrolyte (concentration of the order 0.1 M) is essential. With a double chain surfactant (e.g. Aerosol OT) the cosurfactant can be missed. At increasing concentrations of electrolyte and/or cosurfactant the nature of the microemulsion changes from droplets of oil in water via a presumably bicontinuous pattern to droplets of water in oil. It should be obvious that thermodynamic stability requires the interfacial tension between water and oil to be low (order of $0.01-0.1\ mN\ m^{-1}$) so that the dispersion entropy can offset the interfacial free energy. At these low interfacial tensions the influence of curvature on the interfacial tensions becomes important. It turns out that a given amount of surfactant (and co-surfactant) can only disperse a limited amount of oil in water or of water in oil or of water and oil into one another and therefore a microemulsion may be in equilibrium with non colloidal oil and/or water phases. In the bicontinuous microemulsion oil and water may have a geometrically irregular interface or they may form lamellae of more or less constant thickness or other structures, such as a "molten cubic phase". These equilibria lead to very interesting, but rather complicated phase diagrams. It will be discussed by what mechanisms the various components of the mixture influence the interfacial tension and promote the stability of the microemulsion and how this depends on the chemical nature of the components.

1. Introduction

With the addition of a *small amount of a suitable surfactant* and a great deal of mechanical work (shaking, stirring) oil and water can be emulsified to water in oil (W/O) or oil in water (O/W) emulsions. Such emulsions may exist for a long time, but in the (sometimes very) long run they phase separate into a water and oil layer. They are only kinetically, not thermodynamically stable.

With suitable compositions, containing among other things a *fairly large amount of surfactant* (several %) thermodynamically stable emulsions form (nearly) spontaneously [1]. They are transparent or nearly so, indicating the absence of structures of the size of the wavelength of light or larger, and have been called *microemulsions* [2]. The surfactant may be non-ionic or ionic.

If the *surfactant is ionic* and contains a single hydrocarbon chain (e.g. sodium dodecylsulphate, SDS) microemulsions are only formed if additionally a *cosurfactant* (e.g. a medium size aliphatic alcohol) and *electrolyte* (e.g. 0.2 M NaCl) are present. With *double chain* ionic surfactants (e.g. Aerosol OT, AOT) the presence of a cosurfactant is not necessary.

At low concentrations of cosurfactants and electrolyte O/W microemulsions are formed, which are miscible with more water, but they can contain only a limited amount of oil microdroplets and any more oil will be present as a separate non-colloidal oil phase. At high concentrations of cosurfactant and/or electrolyte W/O microemulsions are formed, miscible with oil but possibly in equilibrium with excess aqueous phase. In between a continuous transition is found from O/W to W/O microemulsions, presumably via bicontinuous dispersions of oil and water [3]. In this middle region the microemulsion may be in equilibrium with both excess oil and excess water. After the author [4] who clearly catalogued them, the three regions (O/W + O, bicontinuous O and W + O + W, W/O + W) are called respectively Winsor I, Winsor III and Winsor II regions. The Winsor I, III, II phase equilibria are frequently denoted by $\underline{2}$, 3, $\bar{2}$, the bar below or above the 2 indicating that the microemulsion is the lower or upper phase respectively. It should be emphasized that the change from O/W via bicontinuous to W/O are not phase transitions with sharp phase boundaries.

The representation of the phase behaviour of ionic microemulsions is complicated due to the relatively large number of components (4 or 5) involved, oil-water-surfactant-(cosurfactant)-salt. In the case of 4 components a tetrahedron is required and in the case of 5 components a graphical representation in three dimensions is impossible. For this reason frequently cuts through the phase diagram are presented, for example at constant water-to-oil ratio or constant surfactant-to-cosurfactant ratio. Another way to simplify the phase diagram is to group components together as a single pseudo component for example water + salt as the pseudo component brine. One must realize that the salt concentration in water in different phases is not the same, due to the negative adsorption of co-ions in the double layer and therefore the use of brine as pseudo component is strictly speaking not correct.

This paper is organized as follows. In the next section we first discuss the crucial role of (extremely) low surface tensions in microemulsions. Then in section 3 we present representative phase diagrams of ionic microemulsions. In Section 4 we give an elementary theory of stability and phase behavior of these microemulsions and in section 5 we study the role of electric double layers associated with the oil-water interfaces loaded with ionic surfactants in the observed phase behaviour and in section 6 we present our conclusions.

  0005-9021/96/0303-0206 $ 15.00+.25/0

2. Low Interfacial Tension

The thermodynamic stability of microemulsions requires the interfacial tension, γ, between oil and water to be very low, so that the interfacial free energy of the droplets can be compensated by the free energy of dispersion (entropy of mixing). For droplets of radius, a, with a free energy of dispersion on the order of a few times kT per droplet (k = Boltzmann constant, T = absolute temperature) this leads to, say

$$3kT \approx 4\pi a^2 \gamma \ . \tag{1}$$

For droplets with a radius of 10 nm this requires the interfacial tension to be on the order of $\gamma \approx 0.01\ \mathrm{mNm}^{-1}$.

The interfacial tension between oil and water is of the order of $50\ \mathrm{mNm}^{-1}$ and it is the role of the surfactants and cosurfactants to lower this interfacial tension to close to zero. Because of the amphipolar nature of surfactants (they contain a polar part and a non polar part, often a fairly long hydrocarbon chain) they are adsorbed spontaneously at the water/oil interface, and this facilitates the extension of the interface, by the lowering of the interfacial tension. Gibbs expressed this quantitatively in the equation (see Adamson [5])

$$\frac{\partial \gamma}{RT \partial \ln c_i} = -\Gamma_i \ , \tag{2}$$

where Γ_i is the amount adsorbed per unit area, c_i is the concentration of the surfactant, R is the gas constant and T the absolute temperature.

In Fig. 1 the interfacial tension, γ, (or surface tension) is plotted against the logarithm of the concentration of a soap or a similar surfactant. According to Eq. (2) the slope of that curve is proportional to the adsorption. At low concentrations the adsorption is small and γ decreases only slowly. At intermediate concentrations the adsorption is often found to be constant, especially in the presence of an excess electrolyte. Obviously the interface is full and *saturation adsorption* is reached [7]. It is a remarkable fact that in the steep part of the curve the surface composition remains virtually constant, whereas the surface tension or interfacial tension changes dramatically. This can be explained by noticing that it requires less work to bring surfactant molecules to the surface from a higher bulk concentration (factor $RT \ln c$ in the free energy of mixing). The interfacial tension decreases rapidly with increasing $\log c$ until, over a very small concentration range, γ becomes virtually constant. Eq. (2) would require the adsorption to fall back to zero, which is utterly improbable. The correct explanation is that Eq. (2) is an approximation. Ln c in the denominator should be ln (activity) and although below the concentration marked cmc activity and concentration are nearly proportional, above it the activity remains constant although the concentration continues to grow. This behavior is explained by the formation of *micelles*, agglomerates of many (e.g. 50) soap molecules. On account of their amphipolar nature, surfactants are in a state of high free energy when individually dispersed and at a certain concentration, the *critical micelle forming concentration* (cmc), the individual molecules associate reversibly to particles that are large enough to hide all the non polar parts from the water with all polar parts at the surface and in contact with the strongly polar water molecules. Above the cmc the concentration of individually dissolved molecules remains constant (or nearly so) and thus the interfacial layer and the interfacial tension remain constant too.

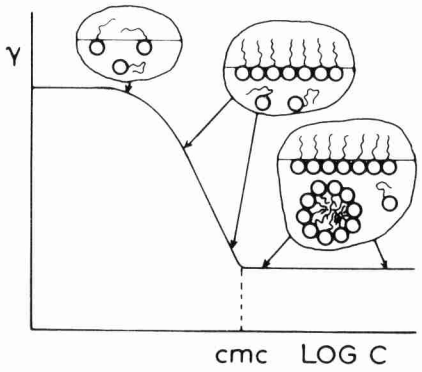

Fig. 1
Surface tension or interfacial tension, γ, plotted against the logarithm of the concentration, c of a surfactant. cmc = critical micelle forming concentration. The polar group of the surfactant is represented as a circle, the hydrocarbon tail as a wavy line. Saturation adsorption often starts at 15–25% of the cmc. (From Overbeek [6])

Back to the low and ultralow interfacial tensions now. Micelle formation usually prevents γ from reaching very low values. But, if a second surfactant, rather different from the first one, is added, then the effects of the two surfactants enhance one another, and the interfacial tension may become extremely low, as illustrated in Fig. 2. The Gibbs Eq. (2) can be extended to the case of the two or more surfactants. It can be written

$$\mathrm{d}\gamma = -\Gamma_1 RT \mathrm{d} \ln c_1 - \Gamma_2 RT \mathrm{d} \ln c_2 \text{ etc.} \tag{3}$$

showing the effects of the two surfactants to be additive, as long as there is not too much interference between the two adsorptions and the concentrations are not spoiled by mixed micelle formation. With a mainly water soluble ionic surfactant and a mainly oil soluble cosurfactant the interfacial tension can become so low that further increase in concentration is not possible without making γ negative. A negative γ would imply that the interface expands spontaneously, taking up the excess of surfactant and cosurfactant, thus bringing γ back to a positive value and in the meantime generating a microemulsion spontaneously. The curve for 20% pentanol in Fig. 2 is a case in point.

It should be mentioned that in a few cases very low interfacial tensions can be reached and microemulsions can be formed with a single surfactant without cosurfactant. This occurs in particular with double chain ionic surfactants [8, 9] and with some non-ionic surfactants [10] in the fairly

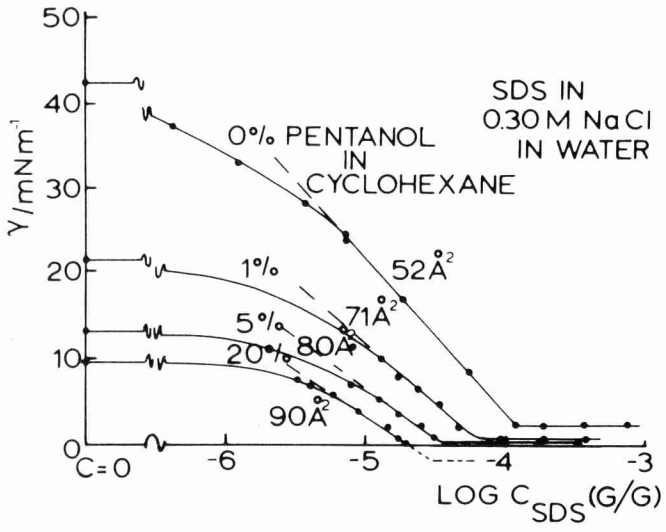

Fig. 2
Interfacial tension between solutions of sodium dodecylsulphate (SDS) in aqueous 0.30 M NaCl and solutions of n-pentanol in cyclohexane. Pentanol (5%) decreases the interfacial tension already to about 13 mNm^{-1}. SDS can then bring the interfacial tension to nearly zero and with 20% pentanol *zero interfacial tension is reached before micelles of SDS in water are formed.* The area per SDS molecule, determined with Eq. (2) increases from 52 $Å^2$ in the absence of pentanol to 90 $Å^2$ with 20% pentanol in the oil phase. (From Overbeek [6])

narrow temperature range where their oil solubility becomes comparable to their water solubility.

Since the surfactant concentration used in preparing microemulsions (several %) is larger than most cmc's ($\ll 1\%$) the final interfacial area in microemulsions is proportional to the amount of surfactant used, but the nature of the microemulsion (O/W, W/O or bicontinuous) does not depend on the amount of surfactant. So long as not yet enough interfacial area has been created to accommodate all available surfactant, some surfactant remains free and the interfacial tension may be negative, thus explaining spontaneous formation of the microemulsion, as is often observed.

With the relatively large surfactant and cosurfactant molecules adsorbed at the interface and considering the strong curvature of the interfaces encountered in microemulsions it should not be unexpected that the curvature affects the interfacial tension significantly and this effect should be taken into account in all considerations on the energetics of microemulsions. In section 4 it will be made clear that the interplay between the hydrocarbon tails of surfactant and cosurfactant, with the charge of the ionic group, the electrolyte concentration and the packing density in the layer, will lead to a preferred radius of curvature, which usually is of the order of nanometers. In the final equilibrium state, based on a minimum in the free energy, to which γ gives a positive contribution and the entropy of mixing a negative one, the interfacial tension will be slightly positive and the droplet size somewhat smaller than the preferred radius because at constant interfacial area then there are more drops and a more negative free energy of mixing.

3. Phases and Phase Diagrams

Given the large number of components – five for oil, water, ionic surfactant, cosurfactant, salt – complete phase diagrams would be multidimensional and hard to draw or describe. Therefore one usually gives suitable cuts through the complete phase diagrams and/or one diminishes the number of components by combining for example water and salt into one quasi-component, brine.

In Fig. 3 phase equilibria are shown, prepared from equal volumes of an aqueous phase (water, ionic surfactant, salt) and an oil phase (oil, cosurfactant). At low salt concentrations O/W microemulsions are found in equilibrium with excess oil; at high salt concentrations one finds W/O microemulsions plus an excess aqueous phase; in between three phase equilibria (W + microemulsion + O) occur at low amounts of surfactant (Fig. 3a) but one phase microemulsions at higher amounts of surfactant (Fig. 3b). Completely similar series of phase equilibria are found at constant concentration of salt but increasing concentrations of cosurfactant.

Upon further increase of the surfactant concentration a first-order transition to a lamellar phase (L_α) may occur. A schematic representation of occurring structures and their variation with surfactant and salt (or cosurfactant) concentration, modeled after Strey [11] and Van Aken [12] is given in Fig. 4.

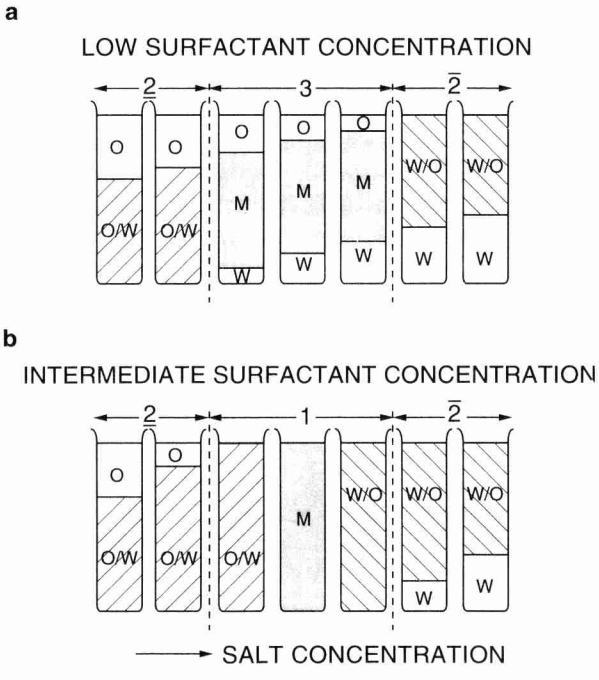

Fig. 3
Schematic illustration of the progression of microemulsion phase equilibria prepared from equal volumes of an aqueous phase (water, ionic surfactant, salt) and an oil phase (oil, cosurfactant) with increasing salinity

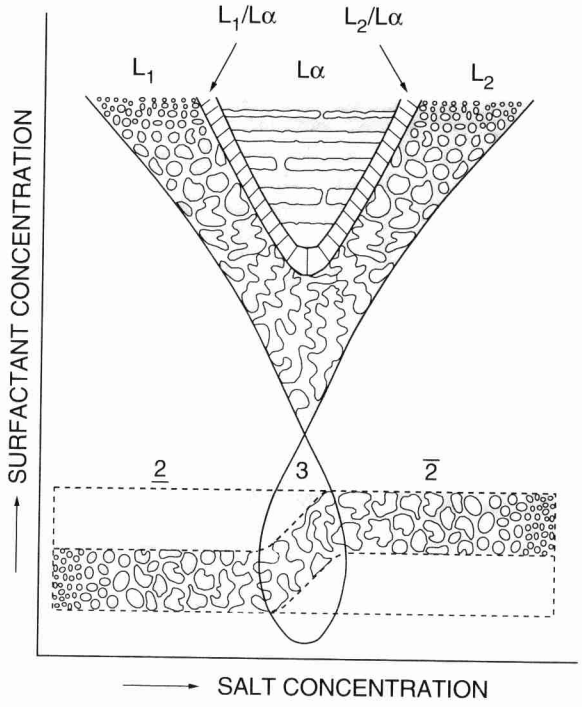

Fig. 4
Schematic representation of occurring structures and their variation with surfactant and salt concentration in a microemulsion system at a water-to-oil ratio of 1. Modeled after Strey [11] and Van Aken [12]. The grey regions represent oil and the white regions brine

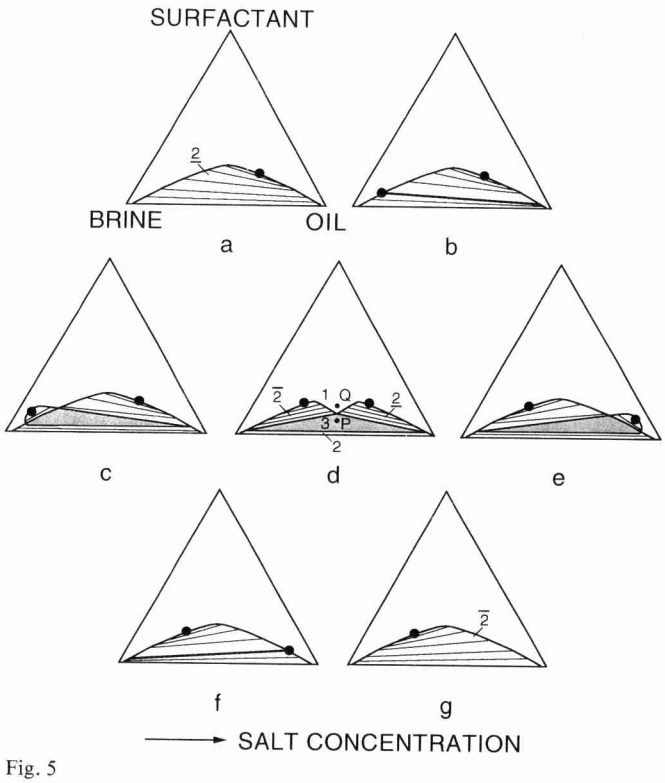

Fig. 5
Schematic representation of the progression of phase behavior as a function of salinity. The critical (end) points are marked with a circle. The critical end point tie lines are marked as thick lines compared to the ordinary tie lines

The phase behavior for a water-to-oil ratio equal to 1 depicted in Fig. 3 can be interpreted in terms of the underlying progression of the phase behavior as a function of salt concentration in the Gibbs composition triangle represented in Fig. 5. The point P represents a system at low surfactant concentration (as in Fig. 3a) and the point Q a system at intermediate salt concentration (as in Fig. 3b). Due to the fact that the two-phase regions 2 and $\bar{2}$ shape a groove at the topcorner of the three-phase triangle, the point Q lies, for the salt concentration corresponding to Fig. 5d, in an one phase region of the phase diagram. For a detailed discussion of this point see [10].

In reality the phase diagrams for ionic microemulsions are not as simple as represented in Fig. 5, due to the fact that we are dealing with more than three components and therefore the representations in Fig. 5 must be considered as pseudo ternary Gibbs phase triangles.

We now show some experimental phase diagrams and first consider microemulsions that contain the double chain anionic surfactant AOT (sodium-bis-ethylhexylsulfosuccinate). This surfactant molecule is one of the most frequently used amphiphiles in model studies of ionic microemulsions. A significant advantage of AOT is that it does not require a cosurfactant to form microemulsions, a feature which considerably simplifies the study and presentation of the phase behaviour of the microemulsions. In Fig. 6 we present the Gibbs phase triangle of the system D_2O (0.6% NaCl)-n-decane-AOT at T = 40 °C.

This diagram closely resembles Fig. 5d, but we stress that Fig. 6 is a pseudo ternary phase diagram with D_2O + NaCl as pseudo component. In fact Fig. 6 must be considered as a cut at constant D_2O/NaCl ratio through the phase dia-

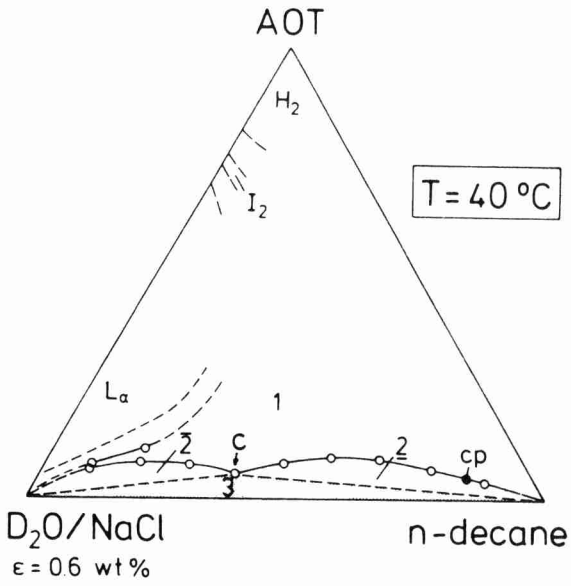

Fig. 6
Gibbs phase triangle D_2O (0.6% NaCl)-n-decane-AOT at T = 40 °C. In addition to the microemulsion phase equilibria $\bar{2}$, 3 and 2, other surfactant phases denoted by L_α (lamellar phase), I_2 (cubic phase), and H_2 (reversed hexagonal phase) are indicated by dotted lines. (From Chen, Chang and Strey [13])

gram in the isothermal composition tetrahedron with vertices D_2O, NaCl, n-decane and AOT. This has as a consequence that tie lines in general do not lie in the plane of Fig. 6 but cut through it. For example increasing the amount of AOT will increase the *activity* of NaCl even though the *concentration* of NaCl is constant. The evolution of the phase behavior of the system AOT-brine-n-decane as a function of salt concentration and surfactant concentration at constant temperature (40 °C) and a water-to-oil ratio equal to 1 is presented in Fig. 7.

Note that the three phase region W + microemulsion + O spans only a fairly narrow salinity range. Clearly the microemulsion phase behavior depends quite sensitively on the salt concentration. This is further exemplified in Fig. 8a where the phase volumes of the system AOT-brine-n-decane as a function of salt concentration at constant AOT concentration (5 wt.% in the aqueous salt solution), constant temperature (30 °C) and a water-to-oil ratio equal to 1 are presented. Now the three phase region W + microemulsion + O spans only a salinity range of approximately 0.01 wt.% NaCl ≅ 0.0016 M. This indicates that under these conditions the three phase region is close to the single phase microemulsion region. Changing the oil component from n-decane to n-dodecane (Fig. 8b) raises both the salt concentration and the salinity range of the three phase region considerably.

We now turn to the phase behaviour of microemulsions with a single chain (an)ionic surfactant which is explained in section 2 require a cosurfactant to form microemulsions, a feature which considerably complicates the study and the presentation of the phase behaviour. Here we shall concentrate on the microemulsions formed with the surfactant SDS (sodium dodecyl sulphate) and medium sized alcohols (butanol, pentanol, hexanol) as cosurfactants. The pioneering work on this system was done by Bellocq and coworkers [16] and it was later studied extensively by Van Nieuwkoop and coworkers [17, 18, 19].

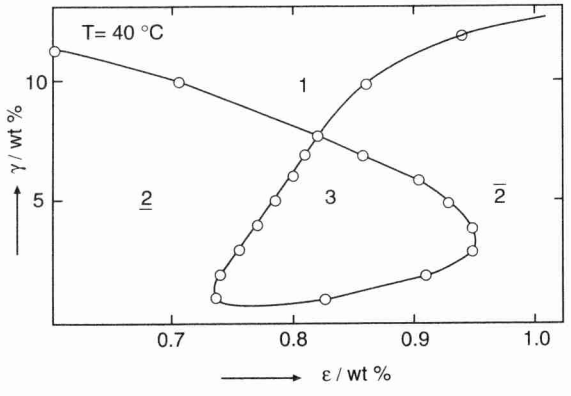

Fig. 7
Three phases body of the quaternary mixture H_2O-n-decane-AOT-NaCl at $T = 40\,°C$ and weight fraction oil in the mixture oil and brine $\alpha = 50\%$, as a function of the amphiphile weight fraction in the mixture of all four components, γ, and of the weight fraction of salt in brine, ε. (Adapted from Kahlweit, Strey, Schomäcker and Haase [14]), courtesy M. Kahlweit)

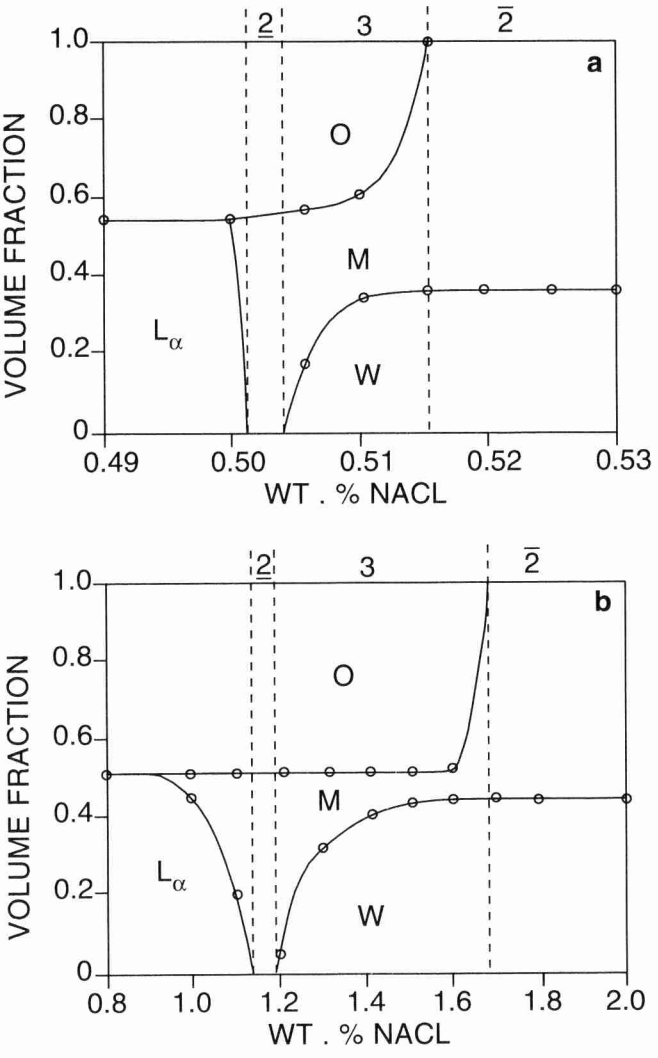

Fig. 8
Volume fractions of the brine (W), oil (O), microemulsion (M) and lamellar (L_α) phase as a function of wt.% NaCl at water-to-oil ratio equal to 1 for (a) the AOT-brine-n-decane system and (b) the AOT-brine-n-dodecane system at $T = 30\,°C$ and 5 wt.% AOT in brine. (From Ghosh and Miller [15])

In Fig. 9a we present the phase tetrahedron of the system SDS-1-butanol-water (6.54 wt.% NaCl)-heptane in Fig. 9b and 9c we present sections of this phase diagram at constant surfactant-to-alcohol ratio and water-to-oil ratio, respectively. The banana shaped three-phase body arises as a result of the "collision" of the two phase regions 2 and 2̄. The intersection with the water-to-oil ratio equal to 1 plane shows the extension of the three-phase body. Again we stress that for the same reason that Fig. 6 is a pseudo ternary phase diagram the representation in Fig. 9a is a pseudo four-component phase diagram. Clearly the situation is more complex than in the case of AOT based microemulsions.

In Fig. 10 we present a schematic representation of a three-phase triangle in the pseudo quaternary system brine-oil-surfactant-alcohol. The tie triangle inside the phase tetrahedron connects the microemulsion with an aqueous

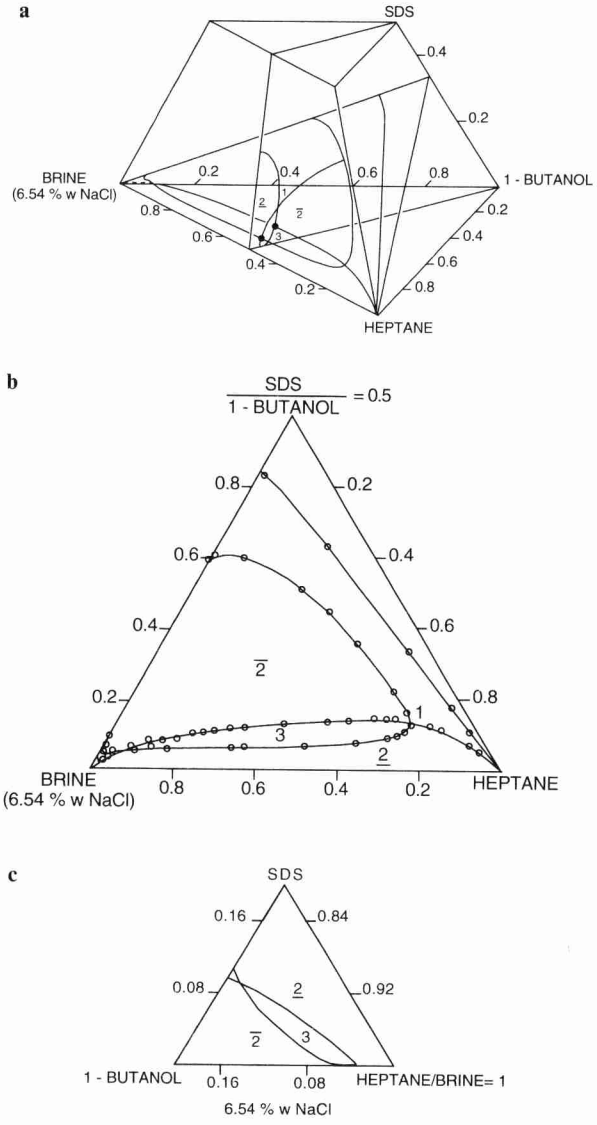

Fig. 9
Phase behavior of the system SDS-1-butanol-brine (6.54 wt.% NaCl)-heptane at 23 °C. a) Pseudo quaternary phase diagram. b) Section at constant surfactant-to-alcohol ratio. c) Section at constant water-to-oil-ratio. (From Van Nieuwkoop and Snoei [17])

and oleic phase located close to the respective corners. Note however that the oleic phase may easily contain 10 – 20% alcohol.

In fact each point inside the three phase body is part of a three phase triangle. For a thorough discussion of the topology of the three phase region in the composition tetrahedron see Widom and Lang [20] and Fox [21]. The evolution of these composition triangles for the interaction of the three phase body with the plane with water-to-oil ratio equal to 1 is schematically represented in Fig. 11.

As noted at the beginning of this section completely similar series of phase equilibria are found on the one hand at constant concentration of salt and increasing concentrations of cosurfactant and on the other hand at constant concentration of cosurfactant and increasing concentration of

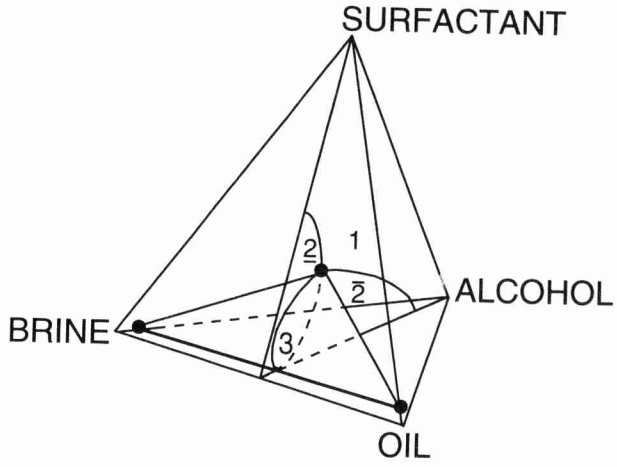

Fig. 10
Schematic representation of a three phase triangle in the pseudo quaternary system brine-oil-surfactant-alcohol

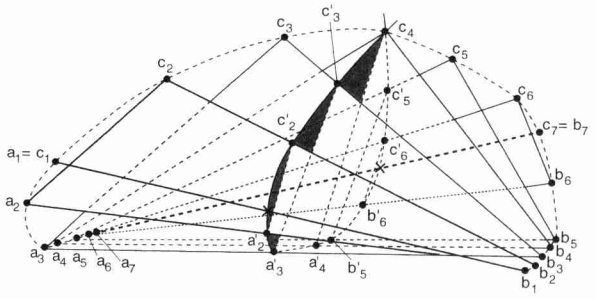

Fig. 11
Schematic representation of an intersection of the water-to-oil ratio equal to 1 plane with the three-phase region in the pseudo quaternary phase diagram. The aqueous phases are denoted by a, the oleic phases by b and the microemulsion phases by c. The three-phase triangles merge into the degenerate triangles $a_1 = c_1$, b_1 and a_7, $c_7 = b_7$. The intersections of the sides of the three-phase triangles with the water-to-oil ratio equal to 1 plane are denoted by a prime. (From Van Nieuwkoop and Snoei [18])

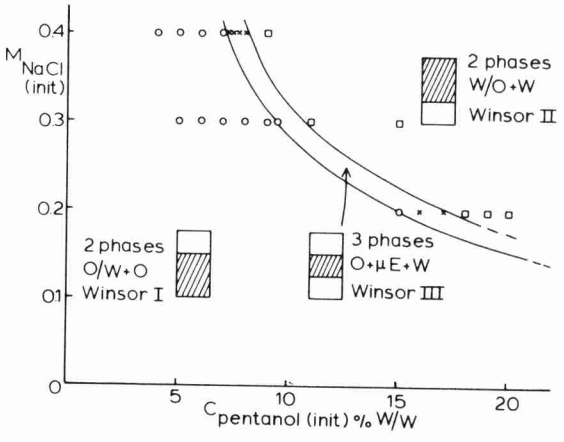

Fig. 12
Different types of phase equilibria after equilibration of 8 g of a solution of pentanol in cyclohexane (pentanol concentration on the horizontal axis) and 10 g of a solution of 1% (w/w) SDS in brine (NaCl concentration on the vertical axis). (From De Bruyn, Overbeek and Verhoeckx [22])

salt. This is illustrated in Fig. 12 for the system aqueous salt solution – cyclohexane-SDS-pentanol.

We finally turn to the role of the type of cosurfactant used [23]. Increasing the chain length of the alcohol used as cosurfactant has a very significant effect on the phase diagram. This is exemplified by the phase diagrams presented in Fig. 13. Here the cosurfactant in the system brine-cyclohexane-SDS-cosurfactant is varied from pentanol to hexanol. This small change causes the lamellar phase to collide with the three phase W + microemulsion + O region giving rise to a four phase equilibrium W + lamellar phase + microemulsion + O. For a discussion of the conditions under which such a four phase equilibrium might be observed in microemulsion system with non-ionic surfactants we refer to [24].

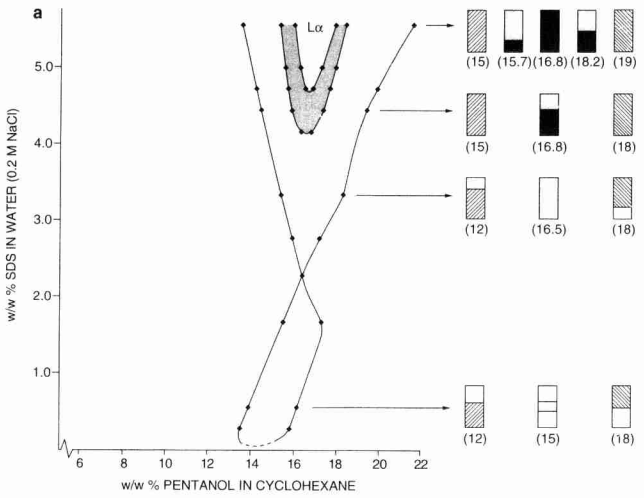

Fig. 13
Phase behaviour of brine (0.2 M NaCl), cyclohexane, SDS and cosurfactant in the SDS-cosurfactant concentration plane with equal volumes of the brine and oil phases as a function of cosurfactant chain length: (a) pentanol; (b) hexanol. The pictograms are on scale representations of the relative volume of the coexisting phases. The cosurfactant concentrations are indicated between parentheses. (From Kegel and Lekkerkerker [23])

4. Elementary Theory of the Stability and Phase Behavior of Ionic Microemulsions [6]

As mentioned briefly in section 2 an ultra low interfacial tension between W and O is essential for the thermodynamic stability of a microemulsion. This low interfacial tension is obtained by the adsorption of the ionic surfactant and the nonionic cosurfactant at the W/O interface. If the concentration(s) of surfactant (and cosurfactant) are (is) sufficiently high, this might drive the interfacial tension temporarily to negative values, which would lead to an extension of the interface, taking up more surfactant and cosurfactant, until nearly all surfactant (and/or cosurfactant) is in the interface. When the concentration goes down further the interfacial tension goes up to positive, but low, values and its positive contribution to the free energy of the system can be offset by the entropy of mixing of the many small droplets formed with the continuous medium.

This mechanism, however, would allow the droplets to take up an infinite amount of liquid, whereas in practice they show only limited swelling, the remainder of the liquid staying behind as a separate phase, (*emulsification failure* [25]), thus giving rise to the Winsor I and II equilibria, O/W + O and W/O + W. To explain this limited swelling, we need to take into account the influence of curvature of the interface on γ, which becomes an important effect at the low interfacial tensions and the strong curvatures of the interfaces of the nanodroplets.

The hydrocarbon chains of surfactant and cosurfactant repel each other, and this promotes curvature of the interface around the water side. The aqueous part of the electric double layer also shows lateral repulsion and thus promotes the formation of oil droplets in water. Addition of an electrolyte, such as NaCl, compresses the double layer (smaller Debye length), decreases the lateral pressure and promotes W/O. The combined effect of the hydrocarbon chains and the electric double layer leads to a *preferred radius* of the interface, usually on the order of nanometers. For a given surfactant, cosurfactant and oil, increase of the concentrations of cosurfactant and/or electrolyte will shift the preferred radius continuously from a value corresponding to a simple surfactant micelle in water via O/W droplets, a flat interface, W/O droplets to inverse micelles in oil.

The total interfacial area being practically fixed by the amount of surfactant available, the entropy of mixing can be increased by having more and smaller droplets. Thus the droplets in microemulsions will be somewhat smaller than the preferred radius. The corresponding increase in interfacial free energy will be more than compensated by the extra entropy of mixing. The entropy of the system can be further increased by having a distribution of droplet sizes rather than by having all droplets of the same size. Size distributions can be estimated reasonably well [26 – 30]. Individual droplets especially the larger ones may be expected to fluctuate in shape, thus leading to more entropy of the system, but quantitative estimates are difficult [31].

An interesting aspect of ionic microemulsions is that the influence of the electric double layer on the interfacial tension and on the bending stress can be calculated quan-

titatively and that these effects show the correct order of magnitude for the droplet sizes present in microemulsions. More details will be given in section 5.

At compositions between the Winsor I and Winsor II regions microemulsions are formed, in which the oil water interfaces are nearly flat, with no preference for curving to the oil or water side, and, in most circumstances, the interfaces are randomly oriented. The most plausible explanation is that we deal here with bicontinuous structures, in which both water and oil are wall to wall continuous. Incidentally at a preferred radius of curvature close to infinity O/W + O and W/O + W equilibria with a size distribution of the droplets could be stable and a rapid transition between the forms of microemulsion might simulate the bicontinuous behavior [29]. These microemulsions take up water and oil, but both only to a limited extent, so that in the Winsor III region three phase equilibria occur, with water, oil and microemulsion. The swelling as such is easily explained because more water and oil allow more or bigger fluctuations of the interfaces with relatively large local radii of curvature. This increases the entropy without undue increase of the interfacial free energy. The question arises however as to why the surfactant rich phase only occupies a limited volume. That the swelling is limited may be due to local Van der Waals attractions where two fluctuating interfaces come close together and the relatively weak attractions are reinforced by small separations and a large area. However, both theoretical [32] and experimental [33] work indicate that due to undulations of the surfactant layers, the net interactions are in general repulsive rather than attractive. A rather successful phenomenological theory [34] considers middle phase microemulsions as ensembles of non-interacting monolayers. These monolayers are characterized by their persistence length [35] which in turn depends exponentially on the bending elastic modulus. The collective character of a middle phase microemulsion is then taken into account by invoking an "entropy of mixing", roughly in the same way as in phenomenological theories of droplet type microemulsions. As a result, the characteristic length scale in the system (the so-called dispersion size) is predicted to be somewhat smaller than the persistence length.

Another explanation for the limited swellability of the middle phase microemulsion may be that the surfactant rich phase does not consist of a more or less independent collection of surfaces but that the system is multiply connected [36]. Experimental indications that middle phase microemulsions resemble a "molten cubic phase" rather than a phase of randomly fluctuating sheets were reported by Strey et al. [37].

As shown in the phase diagrams (Figs. 4 and 13), microemulsions with a lamellar structure are stable close to zero preferred curvature. These lamellar structures can be in equilibrium with random bicontinuous microemulsions and – with hexanol or heptanol as the cosurfactant [23] – simultaneously with excess water and oil. Here it is not clear what mechanism limits the thickness of the water and oil layers, since their thickness is so large (several tens of nm) that Van der Waals attraction seems to be too weak.

So, although, finally we understand the phase behavior of microemulsions reasonably well, there are a few open questions, such as,

a) What is the standard free energy of droplet type microemulsions? Widely different suggestions have been made varying from 0 to minus several times $10\,kT$ [25, 30, 38, 39].
b) How should the fluctuations of the surface of droplets be taken into account?
c) Which mechanism limits the swelling of random and ordered bicontinuous microemulsions?

5. Role of the Electric Double Layer in Microemulsions with Ionic Surfactants

As mentioned in the previous section the lateral repulsion in the electric double layer promotes curvature of the interface around the oil side, the more so the lower the electrolyte concentration, since this results in a longer Debye length ($1/\kappa$) and a thicker double layer. A nice aspect of the electric double layer is that its effecs can be fairly rigorously calculated. Three effects will be considered here.

1. The negative adsorption of co ions leads to a lower salt concentration in the microemulsion phase than in the coexisting aqueous phase. And even when there is no coexisting bulk aqueous phase this effect leads to an increase in the salt activity in the microemulsion phase.
2. As mentioned above, the electric double layer contributes to the bending stress of the oil-water interface. More electrolyte in the aqueous phase promotes change of the curvature of the interface from convex towards water to convex towards oil.
3. The electric double layers of the monolayers interact with each other. For dilute systems with sufficient electrostatic screening this effect may be assumed to be small. However, we shall present experimental data, where that apparently is not the case.

As the starting point for our considerations on the electric double layer we use the Poisson-Boltzmann (PB) equation

$$\nabla^2 \Psi = \kappa^2 \sinh \Psi \,, \tag{4}$$

where Ψ is the dimensionless electric potential

$$\Psi = \frac{e\psi}{kT} \tag{5}$$

and κ is the inverse Debye length

$$\kappa = \left(\frac{2e^2 n_{\text{salt}}}{\varepsilon_r \varepsilon_0 kT} \right)^{1/2} \tag{6}$$

with ψ = electric potential, e = elementary charge, n_{salt} = the number of molecules of uni-uni-valent salt per unit volume, ε_r = the dielectric constant of the solution and

$\varepsilon_0 = 8.8542 \times 10^{-12}\,\mathrm{F\,m^{-1}}$, the permittivity of a vacuum. For low potentials Eq. (4) simplifies to

$$\nabla^2 \Psi = \kappa^2 \Psi \ . \tag{4a}$$

For a flat double layer and a 1-1 electrolyte the exact solution of the PB equation is well-known

$$\tanh\left(\frac{\Psi}{4}\right) = \tanh\left(\frac{\Psi_0}{4}\right) \mathrm{e}^{-\kappa z} \ , \tag{7}$$

where z is the coordinate perpendicular to the surface and Ψ_0 the dimensionless potential at the layer of surface charges. For low potentials Eq. (7) simplifies to

$$\Psi = \Psi_0 \mathrm{e}^{-\kappa z} \ . \tag{7a}$$

When the surface charge density is σ, a convenient dimensionless surface charge density is the quantity

$$p = 2\pi Q \kappa^{-1} \sigma / e = \sinh(\Psi_0/2) \ . \tag{8}$$

Here Q is the so-called Bjerrum length, defined as

$$Q = \frac{e^2}{4\pi k T \varepsilon_0 \varepsilon_r} \ . \tag{9}$$

In aqueous solutions at 25 °C the Bjerrum length $Q = 0.713$ nm. From Eq. (8) it follows immediately that

$$\Psi_0 = 2 \ln(p+q) \tag{10}$$

where

$$q = \sqrt{p^2+1} = \cosh(\Psi_0/2) \ . \tag{11}$$

For low potentials and charge densities Eq. (10) simplifies to

$$\Psi_0 = 2p = 4\pi Q \kappa^{-1} \sigma / e \text{ or } \sigma = e_r \varepsilon_0 \kappa \psi_0 \ . \tag{10a}$$

For the typical charge densities in monolayers of ionic surfactants $|\sigma/e| \cong 1\,\mathrm{nm^{-2}}$, leading to $p \cong 4$ at 0.1 M salt and hence $\Psi_0 \cong 4$ which corresponds to about 100 mV.

5.1 Adsorption of Co-Ions in Electric Double Layers

From Eq. (7) we can easily derive that

$$\frac{\mathrm{d}\Psi(z)}{\mathrm{d}z} = -2\kappa \sinh\left(\frac{\Psi}{2}\right) \ . \tag{12}$$

Using this expression we calculate the negative adsorption of the co-ions in a flat electric double layer as

$$\begin{aligned} \Gamma_{\text{co-ion}} &= c_{\text{salt}} \int_0^\infty [\exp(-\Psi(z)) - 1]\,\mathrm{d}z \\ &= -c_{\text{salt}} \int_{\psi=0}^{\psi_0} \frac{\exp(-\Psi(z)) - 1}{\mathrm{d}\Psi/\mathrm{d}z}\,\mathrm{d}\Psi \\ &= -2\kappa^{-1} c_{\text{salt}} [1 - \exp(-\Psi_0/2)] \ . \end{aligned} \tag{13}$$

For high surface potentials this simplifies to

$$\Gamma_{\text{co-ion}} \cong -2\kappa^{-1} c_{\text{salt}} \ . \tag{14}$$

This means that in a flat double layer with high surface potential (say $\psi_0 \gg 100$ mV) the negative adsorption of co-ions is equal to the amount of co-ions in a layer with a thickness of twice the Debye length.

In the case of microemulsions we are typically dealing with curved interfaces. There is no analytical solution for the PB equation for a curved interface, but in case the curvature is weak an expansion in inverse powers of the reduced radius of curvature κa (a = radius of curvature) can be carried out [40–43]. For the negative adsorption *inside* a highly charged spherical surface this leads to [44]:

$$\Gamma_{\text{co-ion}} = -2\kappa^{-1} c_{\text{salt}} \left(1 - \frac{2}{\kappa a} + \frac{\pi^2/6 - 1}{(\kappa a)^2} + \mathrm{O}\left(\left(\frac{1}{\kappa a}\right)^3\right)\right) \tag{15}$$

Comparison with numerical calculations shows that this expression even for values $\kappa a = 3$ (i.e. Debye length $\kappa^{-1} = \frac{1}{3} a$) leads to quite accurate results. For a discussion of the partitioning of salt in Winsor II systems see [45].

5.2 Contribution of the Electric Double layer to the Bending Stress

The effect of the adsorption layer on the bending stress coefficient (see Eq. (16)) can be split into at least two contributions.

1. The contribution of the electric double layer, including the surface charge and the electrical and concentration (= entropy) effects of all the ions and solvent molecules in the diffuse part (= solution part) of the double layer.
2. All other contributions of the adsorbed surfactant and cosurfactant molecules, in particular those of the hydrocarbon chains.

We know qualitatively that 1. promotes O/W and 2. promotes W/O configurations. The double layer contribution has two aspects:

a) When the interface carrying a double layer is bent around the water side the counter ions are forced together, thus increasing the free energy. Similarly, bending around the oil side will decrease the free energy.
b) On bending the interface the adsorption remains saturated, but it is improbable that the surface of cons-

tant packing coincides with the ionic head groups, since these are not very closely packed, whereas the hydrocarbon tails are. So we expect the surface of close packing somewhere up the chains. As a consequence we expect that the surface charge density (other conditions being equal) will be higher in W/O and lower in O/W situations. For a treatment of this effect, which will not be considered here, see [39].

The electrical contribution to the bending stress coefficient is given as:

$$c_{el} = \left[\frac{\partial F_{el}}{\partial(2/a)}\right]_{p,T,\text{activities}} \tag{16}$$

where

$$F_{el} = \int_0^{\sigma} \psi_0'(\sigma')\,d\sigma' \ . \tag{17}$$

For low charge densities and potentials Eq. (17) simplifies to

$$F_{el}\,(\text{low potentials}) = \frac{1}{2}\psi_0\sigma \tag{17a}$$

The solution of the linearized PB equation

$$\frac{d^2\psi}{dr^2} + \frac{2}{r}\frac{d\psi}{dr} = \kappa^2\psi$$

for an electric double layer inside a sphere with radius a is given by

$$\psi(r) = \psi_0 \frac{a}{r}\frac{\sinh(\kappa r)}{\sinh(\kappa a)} \ , \tag{18}$$

where r is the radial coordinate and $\psi_0 = \psi(r=a)$. The surface charge density is given by

$$\sigma = \varepsilon_r\varepsilon_0\left(\frac{d\psi}{dr}\right)_{r=a} = \psi_0\varepsilon_r\varepsilon_0\kappa\left[\coth(\kappa a) - \frac{1}{\kappa a}\right] \ . \tag{19}$$

For $\kappa a \gg 1$ (thin double layer) this reduces to

$$\sigma = \psi_0\varepsilon_r\varepsilon_0\kappa\left[1 - \frac{1}{\kappa a}\right] \tag{20}$$

and the electric free energy (per unit area) takes the form

$$F_{el} = \frac{1}{2}\frac{\sigma^2}{\varepsilon_r\varepsilon_0\kappa}\left[1 + \frac{1}{\kappa a}\right] \ . \tag{21}$$

In terms of the dimensionless surface charge density p (see Eq. (8)) this can be written as

$$F_{el} = \frac{kTp^2}{2\pi Q\kappa^{-1}}\left[1 + \frac{1}{\kappa a}\right] \ . \tag{22}$$

This leads to a bending stress

$$c_{el} = \frac{kTp^2}{4\pi Q} \ . \tag{23}$$

Although there is no analytical solution for the full PB equation for a curved surface, an expansion in inverse powers of the reduced radius of curvate κa leads to [40–43]

$$F_{el} = \frac{kT}{\pi}(Q^{-1}\kappa)\left[(p\ln(p+q) - q + 1) + \frac{2}{\kappa a}\ln\left(\frac{q+1}{2}\right) + \ldots\right] \ . \tag{24}$$

This leads to a bending stress

$$c_{el} = \frac{kT}{\pi Q}\ln\left(\frac{q+1}{2}\right) \tag{25}$$

which for $p \ll 1$ and hence $q \cong 1 + \frac{1}{2}p^2$ reduces to the result given by Eq. (23). For $|\sigma/e| = 1\,\text{nm}^{-2}$ and electrolyte concentration 0.10 M one finds

$$c_{el} \cong \frac{1\,kT}{\pi Q} \cong 2\times10^{-12}\,\text{N}$$

and for the same surface charge density and electrolyte concentration of 0.4 M one finds

$$c_{el} \cong 0.5\,\frac{kT}{\pi Q} \cong 1\times10^{-12}\,\text{N} \ .$$

The difference between the above values for the electrical contribution to the bending stress of about 1×10^{-12} N typically leads to an inversion of the microemulsion.

5.3 The Interlamellar Spacing as a Function of the Salt Concentration in a 4 Phase System: An Unresolved Question

The interaction free energy per unit area between two flat electric double layers for distances $\kappa D > 2$ is approximately given by [46]

$$\Delta F(D) = F^{el}(D) - F^{el}(\infty) = \frac{8kT}{\pi Q\kappa^{-1}}\left(\frac{p}{q+1}\right)^2\exp(-\kappa D) \ . \tag{26}$$

In the limit of large κD this is a weak interaction. Over the last decade or so it has become clear that the thermal undulations of monolayers and bilayers give rise to an enhanced electric double layer interaction [47 – 51]. In our work [23, 52] on the brine-cyclohexane-SDS-hexanol system we observed large lamellar spacings which we attempted to explain with this enhanced electrostatic repulsion between fluctuating charged monolayers.

The system in which we studied the spacing in a lamellar phase coexisting with a brine, oil and microemulsion phase as a function of the salt concentration consists of SDS, hexanol and equal volumes of brine (with varying salt concentration) and cyclohexane. The salt concentrations were varied in between 0.10 and 0.40 M, and the hexanol concentrations were adjusted in such a way as to keep the system in the 4 phase region. Because of the presence of a large excess phase of water, there is only a negligible effect of a varying effective salt concentration. In Fig. 14 the interlamellar spacings measured by Small Angle X-ray Scattering are plotted as a function of the salt concentration.

It is clear from Fig. 14 that the interlamellar spacing changes dramatically in between 0.1 and 0.3 M NaCl. We note that by comparing the interlamellar spacings with the chemical composition of the lamellar phase, it follows that the thickness of the water layers is about twice that of the oil layers. There is a slight decrease of the water volume fraction in the lamellar phase upon increasing the salt concentration (volume fractions of water are 0.699, 0.699, 0.687 and 0.660 at 0.1, 0.15, 0.20 and 0.30 M NaCl, respectively). In the systems corresponding to Fig. 14, the water spacings (75 nm at 0.2 M) are two orders of magnitude larger than the Debye lengths (0.7 nm at 0.2 M). Therefore electric double layer repulsion, even if enhanced by thermal undulations, appears to be too weak to cause these large water spacings and hence does not explain their variation with salt concentration.

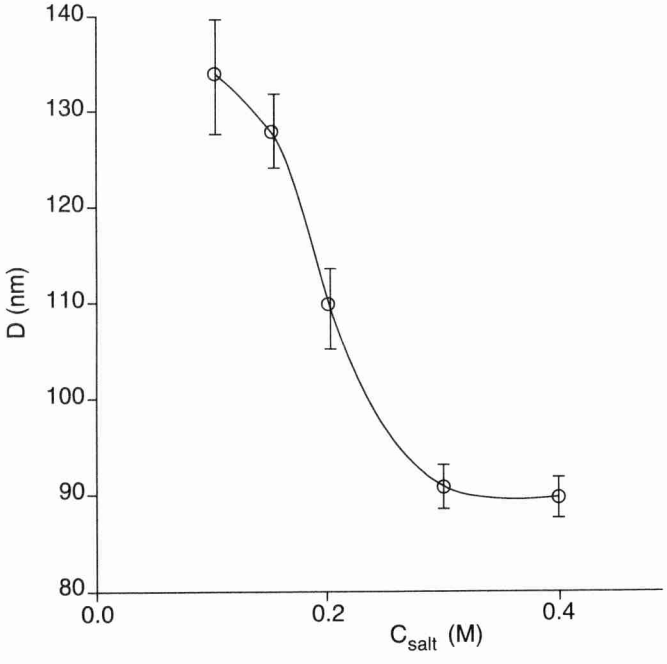

Fig. 14
The interlamellar spacing D in the lamellar phase in the four-phase equilibrium brine-oil-microemulsion-lamellar phase as a function of the salt concentration

6. Conclusion

Ionic microemulsions consist of a relative large number of components (4 or 5), oil-water-surfactant-(cosurfactant)-salt. Great variety of these components leads to great variety of systems, with large differences in detail but with a constant underlying phase behavior pattern. The amount of surfactant determines the total oil-water interfacial area in the system whereas the concentrations of salt and cosurfactant (after adsorption) determine the type of microemulsion (O/W, W/O or bicontinuous). This indicates that the electric double layer bending forces are comparable to steric curvature effects of the hydrocarbon chains.

Although the principles governing ionic microemulsion phase behaviour are well understood i.e. low interfacial tension, influence of bending forces leading to preferred curvature, there are a number of open questions. In particular the mechanism which determines the dispersion size/interlamellar spacing and hence the limited swelling in random and ordered bicontinuous microemulsions is still incompletely understood and requires further work.

We are grateful to Marina Uit de Bulten and Hanneke de Vries for preparing the typescript, to Ingrid van Rooijen for drawing the figures and to Manfred Kahlweit for providing Fig. 7. H.N.W.L. has benefited over the years from the kind and gentle guidance of Reinhard Strey to understand "Die Gleichgewichte der Mikroemulsionen vom Standpunkte der Phasenlehre".

References

[1] T.P. Hoar and J.H. Schulman, Nature *152*, 102 (1943).
[2] J.H. Schulman, W. Stoeckenius, and L.M. Prince, J. Phys. Chem. *63*, 1677 (1959).
[3] L.E. Scriven, Nature *263*, 123 (1976).
[4] P.A. Winsor, Trans. Faraday Soc. *44*, 376 (1948).
[5] A.W. Adamson, Physical Chemistry of Surfaces, p. 68 – 76, 3rd. ed., Interscience, New York 1976.
[6] J.Th.G. Overbeek, Proc. KNAW B *89*, 61 (1986).
[7] F. van Voorst Vader, Trans. Faraday Soc. *56*, 1067; 1078 (1960).
[8] H. Kuneida and K. Shinoda, J. Colloid Interface Sci. *75*, 601 (1980).
[9] S.J. Chen, D. Fennell Evans, and B.W. Ninham, J. Phys. Chem. *88*, 1631 (1984).
[10] M. Kahlweit, R. Strey, and G. Busse, J. Phys. Chem. *94*, 3881 (1990).
[11] R. Strey, Colloid Polym. Sci., Fig. 6, *272*, 1005 (1994).
[12] G.A. van Aken, Proefschrift, Utrecht, A study of Winsor II microemulsion equilibria, 1990.
[13] S.-H. Chen, S.-L. Chang, and R. Strey, J. Chem. Phys. *93*, 1907 (1990).
[14] M. Kahlweit, R. Strey, R. Schomäcker, and D. Haase, Langmuir *5*, 305 (1989).
[15] O. Ghosh and C.A. Miller, J. Phys. Chem. *91*, 4528 (1987).
[16] A.M. Bellocq, J. Biais, B. Clin, A. Gelot, P. Lalanne, and B. Lemanceau, J. Colloid Interface Sci. *74*, 311 (1980).
[17] J. van Nieuwkoop and G. Snoei, J. Colloid Interface Sci. *103*, 400 (1984).

[18] J. van Nieuwkoop and G. Snoei, in: Proceedings of the World Surfactant Congress, Section C-3, Munich, 6 – 10 May 1984.
[19] J. van Nieuwkoop, R.B. Boer, and G. Snoei, J. Colloid Interface Sci., *109*, 350 (1986).
[20] J.C. Lang and B. Widom, Physica A *81*, 190 (1975).
[21] J.R. Fox, J. Chem. Phys. *69*, 2231 (1978).
[22] P.L. de Bruyn, J.Th.G. Overbeek, and G.J. Verhoeckx, J. Colloid Interface Sci. *127*, 244 (1989).
[23] W.K. Kegel and H.N.W. Lekkerkerker, Colloids Surfaces A *76*, 241 (1993); J. Phys. Chem. *97*, 11124 (1993).
[24] R. Strey, Ber. Bunsenges. Phys. Chem. *97*, 742 (1993).
[25] S.A. Safran and L.A. Turkevich, Phys. Rev. Lett. *50*, 1930 (1983).
[26] M. Borkovec, H.-F. Eicke, and J. Ricka, J. Colloid Interface Sci. *131*, 366 (1989).
[27] J.C. Eriksson and S. Ljunggren, Progress Colloid Polymer Sci. *81*, 41 (1990).
[28] J.Th.G. Overbeek, Progress Colloid Polymer Sci. *83*, 1 (1990).
[29] J.Th.G. Overbeek, in: Surfactants in solution, p. 3, ed. by K.L. Mittal and D.O. Shah, Plenum Press, New York 1991.
[30] W.K. Kegel and H. Reiss, This issue of Ber. Bunsenges. Phys. Chem.
[31] W. Helfrich, J. Phys. (France) *47*, 321 (1986).
[32] W. Helfrich, Z. Naturforsch. *33A*, 305 (1978).
[33] D. Roux and C. Safinya, J. Phys. (France) *49*, 307 (1988).
[34] D. Andelman, M.E. Cates, D. Roux, and S.A. Safran, J. Chem. Phys. *87*, 7229 (1987).
[35] P.G. DeGennes and C. Taupin, J. Phys. Chem. *86*, 2294 (1982).
[36] P. Pieruschka and S.A. Safran, J. Phys. Cond. Matter *6*, A357 (1994).
[37] R. Strey, J. Winkler, and L. Magid, J. Phys. Chem. *95*, 7502 (1991).
[38] H. Reiss, J. Colloid Interface Sci. *53*, 61 (1975).
[39] J.Th.G. Overbeek, G.J. Verhoeckx, P.L. de Bruyn, and H.N.W. Lekkerkerker, J. Colloid Interface Sci. *119*, 422 (1987).
[40] S.S. Dukhin, N.M. Semenichin, and L.M. Shapinskaya, Dokl. Phys. Chem. *193*, 540 (1970).
[41] A.N. Stokes, J. Chem. Phys. *65*, 261 (1976).
[42] D.J. Mitchell and B.W. Ninham, Langmuir *5*, 1121 (1989).
[43] H.N.W. Lekkerkerker, Physica A *159*, 319 (1989).
[44] G.A. van Aken, H.N.W. Lekkerkerker, J.Th.G. Overbeek, and P.L. de Bruyn, J. Phys. Chem. *94*, 8468 (1990).
[45] G.A. van Aken, H.N.W. Lekkerkerker, J.Th.G. Overbeek, and P.L. de Bruyn, J. Colloid Interface Sci. *157*, 235 (1993).
[46] E.J.W. Verwey and J.Th.G. Overbeek, Theory of the Stability of Lyophobic Colloids, p. 95, Elsevier Publishing Company, Amsterdam, 1948.
[47] E.A. Evans and V.A. Parsegian, Proc. Natl. Acad. Sci. USA *83*, 7132 (1986).
[48] F. Pincus, J.F. Joanny, and D. Andelman, Europhys. Lett. *11*, 763 (1990).
[49] E. Evans and J. Ipsen, Electrochim. Acta *36*, 1735 (1991).
[50] Th. Odijk, Langmuir *8*, 1690 (1992).
[51] R. de Vries, J. Phys. II (France) *4*, 1541 (1994).
[52] W.K. Kegel, Proefschrift, Utrecht, Interfacial properties and phase behaviour of an ionic microemulsion system, 1993.

Presented at the Discussion Meeting of the Deutsche Bunsen-Gesellschaft für Physikalische Chemie "Microemulsions – Experiment and Theory" in Göttingen, September 4th to September 6th, 1995 E 9106